Pramana – J. Phys. (2019) 92:16
https://doi.org/10.1007/s12043-018-1678-y

Numerical interpretation of autocatalysis chemical reaction for nonlinear radiative 3D flow of cross magnetofluid

W A KHAN[1,*], M ALI[1], F SULTAN[1], M SHAHZAD[1], M KHAN[2] and M IRFAN[2]

[1]Department of Mathematics and Statistics, Hazara University, Mansehra 21300, Pakistan
[2]Department of Mathematics, Quaid-i-Azam University, Islamabad 44000, Pakistan
*Corresponding author. E-mail: waqar_qau85@yahoo.com

MS received 7 January 2018; revised 29 April 2018; accepted 8 June 2018; published online 2 January 2019

Abstract. A simple relation of chemical processes for three-dimensional flow of a cross magnetofluid over bidirectional stretched surface is constructed. The impact of convective heat transport in the manifestation of non-linear thermal radiation and features of heat source–sink are also considered for heat transfer mechanism. Furthermore, in this research paper, the innovative relation between heterogeneous and homogeneous responses with equivalent diffusivities for reactant and autocatalysis is exploited. Apposite alterations are guaranteed to obtain ordinary differential equations (ODEs) with high nonlinearity. Numerically, the bvp4c technique is exploited to the interpret the structure of ODEs. Portrayals of temperature and concentration for cross liquid equivalent to abundant somatic parameters are presented graphically as well as in tabular form. Our results reveal that the temperature of the cross fluid decreases with fluctuation in the heat sink parameter. Furthermore, it is perceived from the figures that the concentration of the cross fluid reduces for higher values of chemical reaction parameters.

Keywords. Three-dimensional flow; cross liquid model; heterogeneous–homogeneous responses; heat source–sink.

PACS Nos **47.10.A−; 47.15.G−, 05.40.Jc; 44.40.+a**

1. Introduction

In chemical mechanisms, the mass transfer process is mainly dependent on the species whose concentration varies. The species varies from low concentrated region to high concentrated region. Chemical processes play a vital role in the innovation of culture and affect life itself. The categorisation of a chemical reaction is specific, and homogeneous and heterogeneous systems are two major systems among them. Homogeneous reactions required the same phase or medium while heterogeneous reactions are through different phase spaces. A homogeneous reaction may be affected by temperature, volume and composition while heterogeneous reactions are more complex in nature due to conflicted phase spaces. A chemical reaction can be identified based on the variety and number of kinetic equations used to draw the progress of the reaction. When a single stoichiometry number and a single kinetic equation are used to complete the chemical progress, then we need a single reaction. Contrary to this, when we apply more than one stoichiometry equation, then more than one kinetic equation is required to observe the changing composition and we have multiple answers. Multiple reactions can be classified into two types: the series reactions and the parallel reactions. Ramzan *et al* [1] presented a mathematical relation to examine the impact of binary reactions and activation energy on magneto-nanofluids. Ramzan *et al* [2] studied the characteristics of chemical processes and double stratification on the radiative flow of Powell–Eyring magnetonanofluids. Shafique *et al* [3] investigated the aspects of activation energy and rotating frame for Maxwell fluid. Khan *et al* [4] analysed the effects of chemical processes on three-dimensional (3D) flow of Burgers fluid. Khan *et al* [5] considered the impact of chemical mechanisms on 3D flow of Burgers fluid. Hayat *et al* [6] inspected the characteristics of melting mechanism and destructive–constructive chemical reactions on magnetohydrodynamics (MHD) flow over stretched surfaces. Khan *et al* [7] deliberated on the homogeneous and heterogeneous reactions on magnetohydrodynamics (MHD) flow in the presence of Joule heating and viscous dissipation. Ramana Reddy *et al* [8] explored

the features of radiation aspects of rotating plates in the presence of chemical mechanisms. Animasaun *et al* [9] analysed the impact of induced MHD for homogeneous and heterogeneous reactions in the presence of nonlinear thermal radiation. Khan *et al* [10] addressed analytically the properties of Maxwell fluid by utilising heat sink–source and homogeneous–heterogeneous reaction aspects. Khan *et al* [11] computed the stretched flow by considering the generalised Burgers fluid with chemical processes. Mustafa *et al* [12] examined the characteristics of activation energy and chemical mechanisms on the magnetonanofluids. Sohail *et al* [13] explained the chemical processes and heat conduction for viscoelastic fluids. Mahanthesh *et al* [14] investigated the aspects of chemical reaction on 3D flow of nanoliquids. Khan *et al* [15] reported the analytical study of Maxwell liquid by utilising the aspects of chemical mechanisms. Khan *et al* [16] discussed numerically the thermophysical properties of unsteady flow of Carreau fluid in the presence of chemical reacting species.

Radiation is a mechanism in which electromagnetic waves spread from hot surface to its adsorption point. Radiation is a significant component in the treatment of various malignancies. Moreover, technological applications of thermal radiation can be seen in nuclear power plants, solar power technology, chemical processes and combustion chambers. Moreover, radiative heat transport law of Stefan–Boltzmann states that energy emitted by a hot surface is directly proportional to the fourth power of the surface's absolute temperature. It has been observed that when the temperature difference between the object and free stream fluid is large, thermal radiation is capable of inverting the thermal boundary layers and related rate of heat transfer. Moreover, in the literature, investigators utilised the linear radiation aspects, which are valid only for small temperature differences. Therefore, it is challenging to construct systems of engineering applications in which liquids have small temperature differences. Thus, investigators were interested to consider nonlinear thermal radiation aspects because nonlinear thermal radiation provides large temperature difference. Khan *et al* [17] developed mathematical relation for 3D radiative flow of Burgers nanofluid by considering the aspects of newly suggested max flux conditions. Farooq *et al* [18] discussed the effect of nonlinear thermal radiation with MHD stagnation point flow of viscoelastic nanofluids. Atlas *et al* [19] investigated the impact of radiation on nanoliquids by considering the squeezing channels and zero flux relations. Akbar and Khan [20] examined the aspects of thermal radiation and slip mechanisms on the nanofluids. Hayat *et al* [21] deliberated on the characteristics of chemical reactions on magneto-Jeffrey liquid in the presence of nonlinear thermal radiation. Khan *et al* [22] considered the impact of chemical processes and radiation phenomenon on viscous liquids. Nayak *et al* [23] deliberated on the features of 3D magnetonanofluid by utilising the aspects of thermal radiation. Nayak [24] investigated the impact of viscous dissipation on magnetonanoliquids. Waqas *et al* [25] addressed the characteristics of nonlinear thermal radiation for slendering surface by considering the aspects of thermophoresis and Brownian diffusion. Sandeep and Gnaneswara Reddy [26] analysed the impact of copper nanoparticles on water by considering different geometries. Mahanthesh *et al* [27] deliberated on the features of nonlinear 3D stretched flow for Oldroyd-B fluid. Bhatti *et al* [28] investigated the heat transfer mechanism for MHD particle–fluid suspension under the influence of thermal radiation induced by metachronal wave.

Nowadays, rheology of non-Newtonian fluid [29–37] mechanisms has gained substantial attention among investigators because of their growing industrial and technical importance in petroleum, polymer and food processing industries. Such mechanisms of non-Newtonian fluid cannot be characterised just like Newtonian fluids. Because of disparity of flow in nature, numerous fluid relations have been suggested by investigators to explore the physical properties of these fluids. Out of these models, the cross fluid model is a subclass of generalised Newtonian fluids. Furthermore, the cross fluid model is significant in the preparation of various polymer solutions. Manzur *et al* [38] investigated the aspects of thermal radiation for the cross fluid in the presence of buoyancy assisting and opposing flows.

Inspired by such realities, this study aims at exploring the characteristics of heterogeneous and homogeneous responses on 3D steady cross magnetofluid over a bidirectional stretched surface. The influence of nonlinear thermal radiation with the features of heat sink–source and convective heat transport are also inspected for heat transfer mechanism. Numerical elucidation is realised for the existent flow problem by utilising bvp4c. The graphical depiction of diverse noticeable considerations on cross liquid temperature and concentration profiles with essential aspect is also an aspect scrutinised in this study. An assessment to former exploration is also provided to authenticate the acquired outcomes.

2. Problem formulation

We considered the unsteady 3D flow of a cross magnetoliquid in the presence of convective heat transport over a bidirectional stretched surface with velocities $U_w(x,t)$ and $V_w(y,t)$, respectively, in which x is the coordinate measured besides the sheet (see

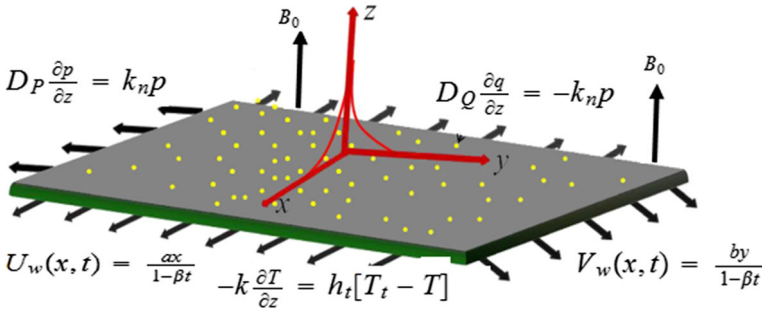

Figure 1. The physical geometry of the problem.

figure 1). Heat transfer exploration is carried out in the manifestation of nonlinear thermal radiation and heat source–sink. Additionally, the flow analysis is executed with heterogeneous and homogeneous responses. A magnetic field is applied along the z-axis. Because of the small magnetic Reynolds number, the induced magnetic field is discounted. Moreover, a conjecture is prepared that the intense liquid below the sheet with temperature T_t transforms the sheet temperature by convective heat transference approach, which delivers the coefficient of heat transfer h_t. The homogeneous response for cubic autocatalysis can be written as

$$P + 2Q \to 3Q, \text{ rate} = k_m pq^2, \tag{1}$$

while on the surface catalyst, the first-order isothermal response is

$$P \to Q, \text{ rate} = k_n p, \tag{2}$$

where P, Q, p, q, k_m, k_n are, respectively, the chemical species, concentration of the species and rate constants. Moreover, the concentration of the reactant P at infinity is p_0 while the concentration of the reactant Q at infinity is zero and these reactions are isothermal.

By utilising the above-mentioned assumptions, the flow problem with boundary conditions is stated as

$$\frac{\partial u}{\partial x} + \frac{\partial v}{\partial y} + \frac{\partial w}{\partial z} = 0, \tag{3}$$

$$\frac{\partial u}{\partial t} + u\frac{\partial u}{\partial x} + v\frac{\partial u}{\partial y} + w\frac{\partial u}{\partial z} = -\frac{1}{\rho_f}\frac{\partial p_1}{\partial x} + \nu\partial/\partial z\left[\frac{\partial u/\partial z}{1+\{\Gamma\,(\partial u/\partial z)\}^n}\right] - \frac{\sigma B_0^2 u}{\rho_f}, \tag{4}$$

$$\frac{\partial v}{\partial t} + u\frac{\partial v}{\partial x} + v\frac{\partial v}{\partial y} + w\frac{\partial v}{\partial z} = -\frac{1}{\rho_f}\frac{\partial p_1}{\partial y} + \nu\frac{\partial}{\partial z}\left[\frac{\partial v/\partial z}{1+\{\Gamma\,(\partial v/\partial z)\}^n}\right] - \frac{\sigma B_0^2 v}{\rho_f}, \tag{5}$$

$$\frac{\partial T}{\partial t} + u\frac{\partial T}{\partial x} + v\frac{\partial T}{\partial y} + w\frac{\partial T}{\partial z} = \alpha_1\frac{\partial^2 T}{\partial z^2} - \frac{1}{(\rho c)_f}\frac{\partial q_r}{\partial z} + \frac{Q_0}{(\rho c)_f}(T - T_\infty), \tag{6}$$

$$\frac{\partial p}{\partial t} + u\frac{\partial p}{\partial x} + v\frac{\partial p}{\partial y} + w\frac{\partial p}{\partial z} = D_P\frac{\partial^2 p}{\partial z^2} - k_m pq^2, \tag{7}$$

$$\frac{\partial q}{\partial t} + u\frac{\partial q}{\partial x} + v\frac{\partial q}{\partial y} + w\frac{\partial q}{\partial z} = D_Q\frac{\partial^2 q}{\partial z^2} + k_m pq^2. \tag{8}$$

The boundary conditions of the flow problem are:

$$u = U_w(x,t) = \frac{ax}{1-\beta t},$$

$$v = V_w(x,t) = \frac{by}{1-\beta t}, \quad w = 0,$$

$$-k\frac{\partial T}{\partial z} = h_t[T_t - T], \quad D_P\frac{\partial p}{\partial z} = k_n p,$$

$$D_Q\frac{\partial q}{\partial z} = -k_n p \quad \text{at } z = 0, \tag{9}$$

$$u \to 0, \quad v \to 0, \quad T \to T_\infty, \quad p \to p_0,$$

$$q \to 0 \text{ as } z \to \infty, \tag{10}$$

where $u, v, w, T, C, \nu, \Gamma, n, \rho_f, p_1, \alpha_1, q_r, D_P, D_Q$ are the velocity components in the x, y and z directions, temperature, concentration, kinematic viscosity, fluid parameters, material time constant or consistency index, fluid density, pressure, thermal diffusivity of base liquid, radiative heat flux and diffusion species coefficients of P and Q, respectively.

The expression of radiative heat flux q_r is simplified as

$$q_r = -\frac{4\sigma^*}{3k^*}\frac{\partial T^4}{\partial z} = -\frac{16\sigma^* T^3}{3k^*}\frac{\partial T}{\partial z}, \tag{11}$$

where σ^* and k^* are the Stefan–Boltzmann constant and coefficient of mean absorption, respectively.

In view of overhead manifestation in eq. (6), we get

$$\frac{\partial T}{\partial t}+u\frac{\partial T}{\partial x}+v\frac{\partial T}{\partial y}+w\frac{\partial T}{\partial z}=\alpha_1\frac{\partial^2 T}{\partial z^2}+\frac{16\sigma^*}{3k^*(\rho c)_f}\frac{\partial}{\partial z}\left(T^3\frac{\partial T}{\partial z}\right). \tag{12}$$

The following pertinent conversions are

$$\begin{aligned}
u&=\frac{ax}{1-\beta t}f'(\eta),\\
v&=\frac{ay}{1-\beta t}g'(\eta),\\
w&=-\sqrt{\frac{a\nu}{1-\beta t}}[f(\eta)+g(\eta)],\\
\theta(\eta)&=\frac{T-T_\infty}{T_t-T_\infty},\\
p&=p_0 I(\eta),\\
q&=q_0 e(\eta),\\
\eta&=z\sqrt{\frac{a}{\nu(1-\beta t)}}.
\end{aligned} \tag{13}$$

In view of the above conversions, the condition of incompressibility is satisfied automatically and eqs. (4)–(10) yield

$$\left[1+(1-n)\left(\mathrm{We}_1 f''\right)^n\right]f'''-\left[1+\left(\mathrm{We}_1 f''\right)^n\right]^2\times[f'^2-(f+g)f'']-\left[S\left(f'+\frac{1}{2}\eta f''\right)+M^2 f'\right]\times\left[1+\left(\mathrm{We}_1 f''\right)^n\right]^2=0, \tag{14}$$

$$[1+(1-n)\left(\mathrm{We}_2 g''\right)^n]g'''-\left[1+\left(\mathrm{We}_2 g''\right)^n\right]^2\times\left[g'^2-(f+g)g''\right]-\left[S\left(g'+\frac{1}{2}\eta g''\right)+M^2 g'\right]\times\left[1+\left(\mathrm{We}_2 g''\right)^n\right]^2=0, \tag{15}$$

$$\frac{\mathrm{d}}{\mathrm{d}\eta}\left[\left\{1+R_d(1+(\theta_f-1)\theta)^3\right\}\theta'\right]-\frac{\mathrm{Pr}\,S}{2}\eta\theta'+\mathrm{Pr}(f+g)\theta'+\mathrm{Pr}\,\delta\theta=0, \tag{16}$$

$$\frac{1}{\mathrm{Sc}}I''-\frac{S}{2}\eta I'+(f+g)I'-k_1 I e^2=0, \tag{17}$$

$$\frac{\lambda_1}{\mathrm{Sc}}e''-\frac{S}{2}\eta e'+(f+g)e'+k_1 d e^2=0, \tag{18}$$

$$\begin{aligned}
&f(0)=0,\quad g(0)=0,\\
&f'(0)=1,\quad g'(0)=\alpha,\\
&\theta'(0)=-\gamma[1-\theta(0)],\\
&I'(0)=k_2 I(0),\quad e'(0)=-k_2 I(0),\\
&f'\to 0,\quad g'\to 0,\quad \theta\to 0,\quad I\to 1,\\
&e\to 0\quad \text{as } \eta\to\infty.
\end{aligned} \tag{19, 20}$$

In the above expressions, We_1, We_2, M, S, α, γ, R_d, θ_f, Pr, δ, λ_1, k_1, k_2, Sc are the local Weissenberg numbers, magnetic parameter, unsteadiness parameter, ratio of stretching rate parameter, Biot number, radiation parameter, temperature ratio parameter, Prandtl number, heat source–sink parameter, ratio of diffusion coefficient, measures the strength of heterogenous–homogeneous processes, respectively. Mathematically, these parameters are expressed in the following manner:

$$\begin{aligned}
&\mathrm{We}_1=\sqrt{\frac{\Gamma a U_w^2}{\nu(1-\beta t)}},\quad \mathrm{We}_2=\sqrt{\frac{\Gamma a V_w^2}{\nu(1-\beta t)}},\\
&R_d=\frac{16\sigma^* T_\infty^3}{3kk^*},\quad \alpha=\frac{b}{a},\quad \theta_f=\frac{T_t}{T_\infty},\quad S=\frac{\beta}{a},\\
&M^2=\frac{\sigma B_0^2(1-\beta t)}{\rho_f a},\quad \gamma=\frac{h_f}{k}\sqrt{\frac{\nu}{a}},\quad \mathrm{Pr}=\frac{\nu}{\alpha_1},\\
&\delta=\frac{Q_0(1-\beta t)}{a(\rho c)_f},\quad \lambda_1=\frac{D_Q}{D_P},\quad \mathrm{Sc}=\frac{\nu}{D_P}.
\end{aligned} \tag{21}$$

For simplicity, we assumed that diffusion coefficients D_P and D_Q are equal and thus we have the following relation:

$$I(\eta)+e(\eta)=1. \tag{22}$$

Now, consequently, eqs (17) and (18) yield

$$\frac{1}{\mathrm{Sc}}I''-\frac{S}{2}\eta I'+(f+g)I'-k_1(1-I)^2 I=0 \tag{23}$$

with boundary conditions

$$I'(0)=k_2 I(0),\quad I\to 1\quad \text{as } \eta\to\infty. \tag{24}$$

3. Physical quantities

Chemical and physical quantities of interest in this research work are the skin friction coefficients and rate of heat transfer. The expressions for the skin friction coefficients and local Nusselt number are given as follows:

$$\begin{aligned}
C_{f_x}&=\frac{2\tau_{xz}}{\rho_f U_w^2},\quad C_{f_y}=\frac{2\tau_{yz}}{\rho_f U_w^2},\\
\mathrm{Nu}_x&=-\frac{x}{(T_t-T_\infty)}\left(\frac{\partial T}{\partial z}\right)\Big|_{z=0}+\frac{xq_\mathrm{r}}{k(T_t-T_\infty)}.
\end{aligned} \tag{25}$$

The above quantities are in the dimensionless form, and we have

Table 1. Numerical values of local skin friction coefficients $\frac{1}{2}C_{f_x}(\mathrm{Re}_x)^{1/2}$ and $\frac{1}{2}(U_w/V_w)C_{f_y}(\mathrm{Re}_y)^{1/2}$ for distinct values of escalating parameters.

We_1	α	We_2	n	M	$\frac{1}{2}C_{f_x}(\mathrm{Re}_x)^{1/2}$	$\frac{1}{2}(U_w/V_w)C_{f_y}(\mathrm{Re}_y)^{1/2}$
2.0	0.8	2.0	0.8	0.9	0.27753248	−0.14803322
3.0	–	–	–	–	0.19243895	−0.29145241
4.0	–	–	–	–	0.12341051	−0.30707752
–	0.0	–	–	–	0.15735507	0.30159281
–	0.4	–	–	–	0.12832017	0.044875384
–	0.7	–	–	–	0.10608653	0.026671393
–	–	1.9	–	–	0.25189512	−0.029730894
–	–	3.0	–	–	0.27466712	−0.24505916
–	–	4.0	–	–	0.30361253	0.15849571
–	–	–	0.2	–	−1.372597	−1.1462287
–	–	–	0.5	–	−0.73602615	−0.6879723
–	–	–	0.7	–	−0.011940978	−0.17751861
–	–	–	–	0.0	0.11808658	−0.16286007
–	–	–	–	0.3	0.15934816	−0.28413843
–	–	–	–	0.4	0.16838717	−0.63312652

$$\frac{1}{2}C_{f_x}(\mathrm{Re}_x)^{1/2} = \frac{f''(0)}{\left[1+(\mathrm{We}_1 f''(0))^n\right]},$$
$$\frac{1}{2}\left(\frac{U_w}{V_w}\right)C_f(\mathrm{Re}_y)^{1/2} = \frac{g''(0)}{\left[1+(\mathrm{We}_1 g''(0))^n\right]},$$
$$\mathrm{Re}_x^{-1/2}\mathrm{Nu}_x = -[1+R_d\{1+(\theta_f-1)\theta(0)\}^3]\theta'(0)\,, \tag{26}$$

in which $\mathrm{Re}_x = ax^2/\nu$ is the local Reynold number.

4. Graphical outcomes and discussion

In this research work, numerical solutions are accomplished for the analysis of constructive–destructive aspects of MHD 3D forced convective flow of the cross fluid. Heat source–sink and nonlinear radiation effects are taken into consideration. The governing ODEs and boundary conditions are analysed by utilising the bvp4c function in Matlab. Detailed graphical analysis has been made for the temperature and concentration fields and discussed for various parameters of interest. Furthermore, skin friction coefficients for fluctuating parameters are characterised in table 1. From table 1, we perceived that skin friction coefficient enriches for accumulative values of M and We_2 while it illustrates the diminishing behaviour of We_1 and n. The rate of heat transfer for fluctuation of various parameters is included in table 2. It is detected from table 2 that the rate of heat transfer decreases for higher values of M while the rate of heat transfer increases for larger values of R_d, γ and Pr for both shear thinning and thickening cases.

Table 2. Numerical values of the local Nusselt number for different parameters when $\mathrm{We}_1 = \mathrm{We}_2 = 2.0$, $\alpha = 0.3$, $\delta = 0.2$, $\theta_f = 1.2$ and $\mathrm{Pr} = 2.0$ are fixed.

S	M	R_d	γ	Pr	$\mathrm{Nu}_x\mathrm{Re}_x^{-1/2}$	
					$n = 0.5$	$n = 1.5$
0.3	0.5	0.3	0.5	2.0	0.411062	0.429949
0.4	–	–	–	–	0.424277	0.439151
0.5	–	–	–	–	0.435556	0.447557
0.6	–	–	–	–	0.445239	0.455161
0.3	0.0	1/Nx3	1/Nx3	1/Nx3	0.418642	0.433624
–	0.2	–	–	–	0.417404	0.433017
–	0.4	–	–	–	0.413749	0.431242
–	0.5	0.0	–	–	0.324812	0.337217
–	–	0.4	–	–	0.438037	0.459293
–	–	0.8	–	–	0.537834	0.569123
–	–	0.3	0.1	–	0.116831	0.118229
–	–	–	0.2	–	0.211790	0.216517
–	–	–	0.4	–	0.355621	0.369532
–	–	–	0.5	1.0	0.328768	0.352512
–	–	–	–	1.3	0.360871	0.383626
–	–	–	–	1.7	0.392740	0.413299

4.1 *Temperature field*

The temperature profiles of cross fluid exhibit remarkable changes with the variation of R_d, θ_f, δ, M and γ for $n < 1$ and $n > 1$. The variation of temperature profile with these parameters is illustrated in figures 2–7. Figures 2a, 2b and 3a, 3b present the impact of R_d and θ_f on the temperature profile of the cross fluid. These figures show that augmented values of R_d and θ_f affect the heat transfer strongly. It can be seen from the figures that the temperature of the

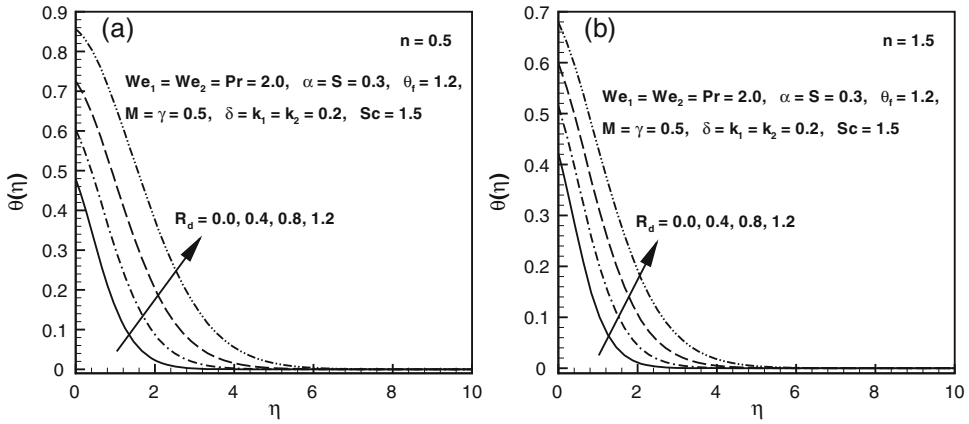

Figure 2. Influence of R_d on $\theta(\eta)$ for (**a**) shear-thinning and (**b**) shear-thickening liquids.

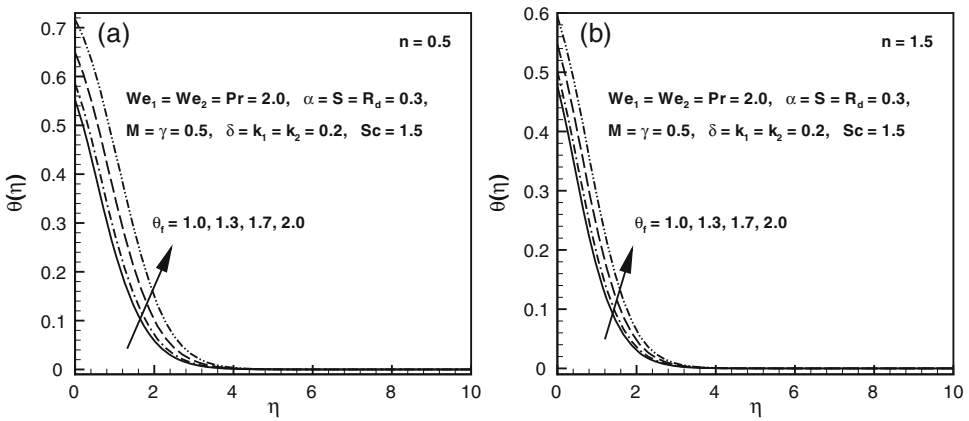

Figure 3. Influence of θ_f on $\theta(\eta)$ for (**a**) shear-thinning and (**b**) shear-thickening liquids.

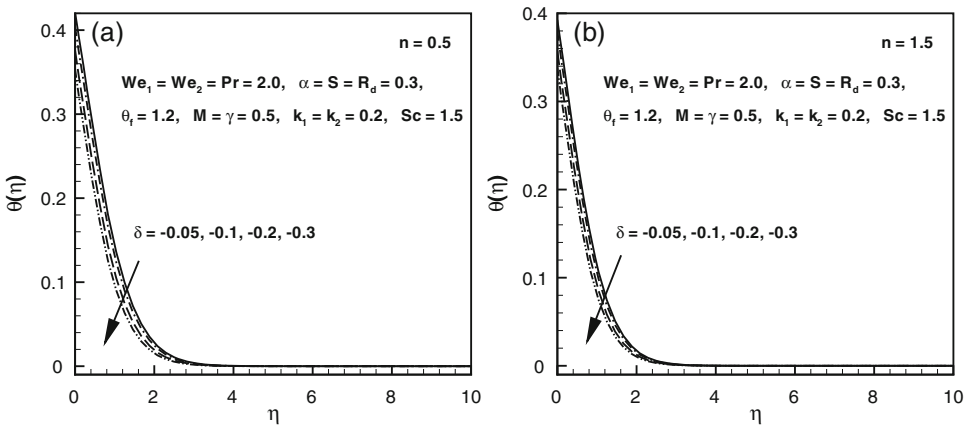

Figure 4. Influence of heat sink ($\delta < 0$) on $\theta(\eta)$ for (**a**) shear-thinning and (**b**) shear-thickening liquids.

cross fluid increases for augmented values of R_d and θ_f. Physically, as θ_f strengthens, the temperature of the cross fluid at the wall becomes higher compared to the temperature of the cross liquid at infinity. As a result, the temperature of the fluid increases. To exhibit the effects of heat source–sink on the temperature profile of the cross fluid, we have plotted figures 4a, 4b and 5a, 5b. These figures show that the temperature of the cross fluid decreases for $\delta < 0$ while the reverse trend is detected for $\delta > 0$. Physically, the heat source parameter provides more heat to the cross fluid due to which the temperature of the cross fluid intensifies. Figures 6a, 6b and 7a, 7b

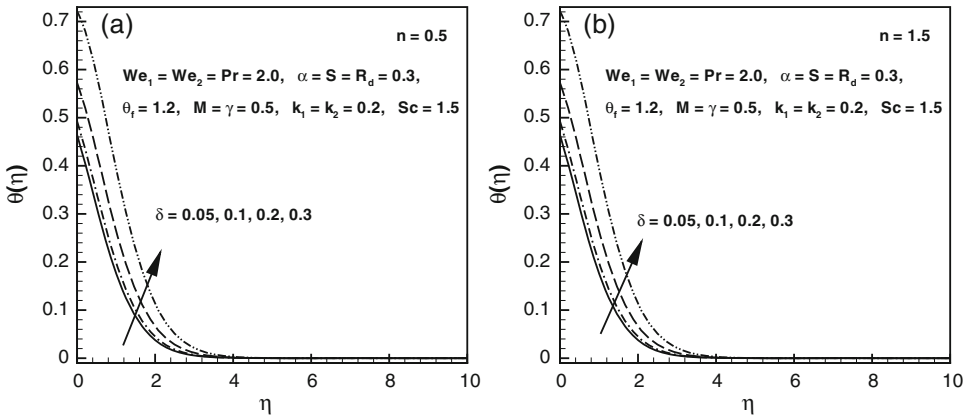

Figure 5. Influence of heat source ($\delta > 0$) on $\theta(\eta)$ for (**a**) shear-thinning and (**b**) shear-thickening liquids.

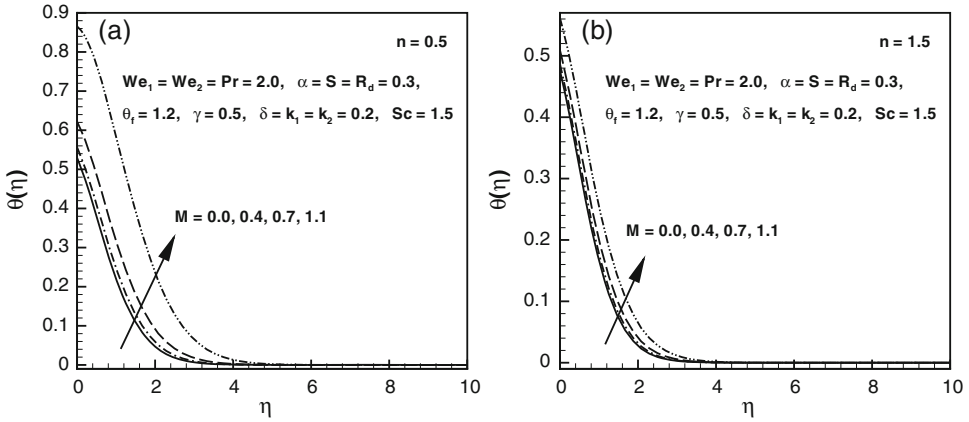

Figure 6. Influence of M on $\theta(\eta)$ for (**a**) shear-thinning and (**b**) shear-thickening liquids.

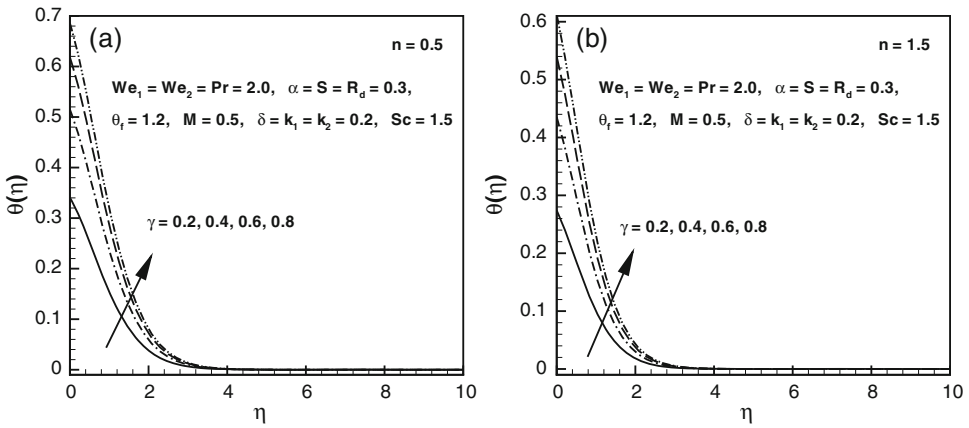

Figure 7. Influence of γ on $\theta(\eta)$ for (**a**) shear-thinning and (**b**) shear-thickening liquids.

interpret the dependence of the magnetic parameter M and Biot number γ on cross fluid temperature for $n < 1$ and $n > 1$. It can be seen from the graphical data that cross fluid temperatures increase with the augmented values of these physical parameters. Physically, as we enrich M, Lorentz's force increases due to which collision between the particles of the cross fluid enhances. As a result, the temperature of the cross fluid rises. Additionally, from these figures the dominant effect of M for cross fluid temperature is detected for $n < 1$. Furthermore, the physical reason behind this trend of γ is that less resistance is faced by the thermal wall which causes an enhancement in convective heat transfer to the fluid.

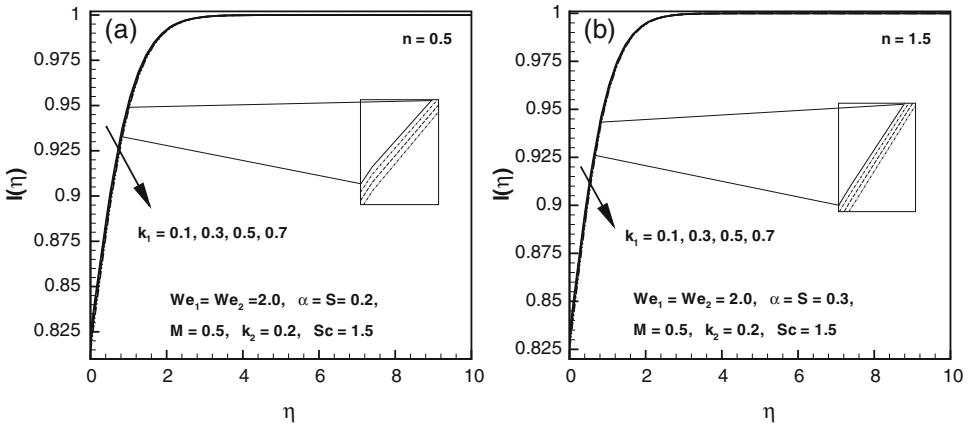

Figure 8. Influence of k_1 on $I(\eta)$ for (**a**) shear-thinning and (**b**) shear-thickening liquids.

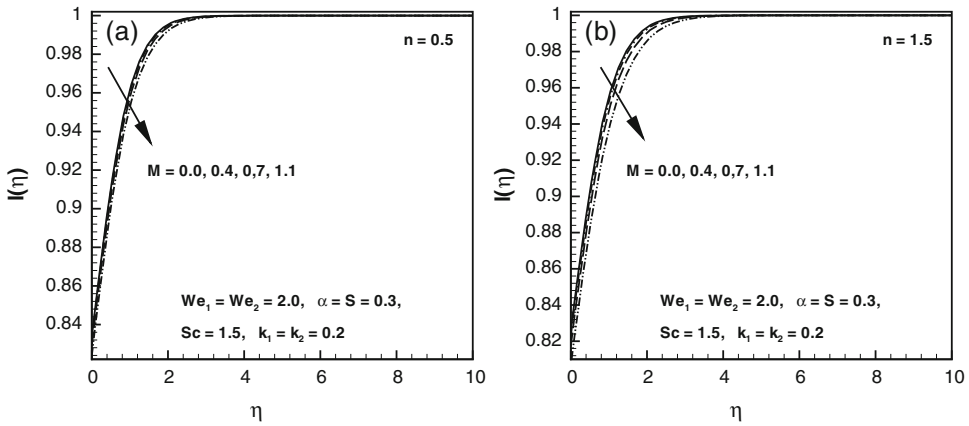

Figure 9. Influence of M on $I(\eta)$ for (**a**) shear-thinning and (**b**) shear-thickening liquids.

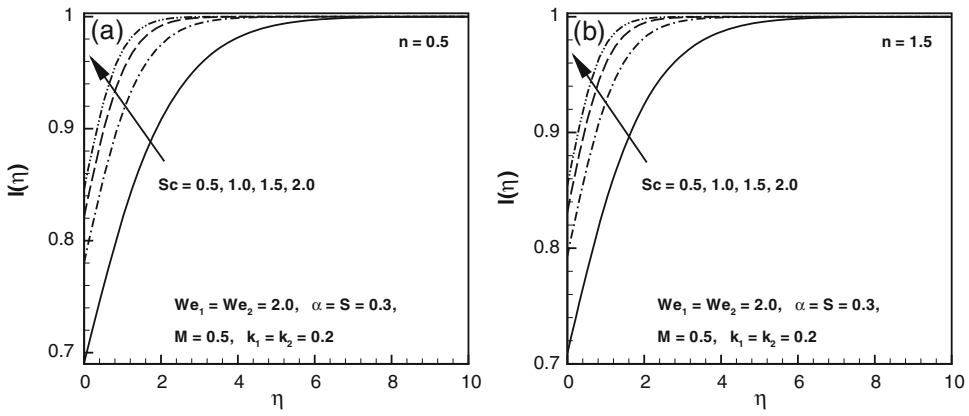

Figure 10. Influence of Sc on $I(\eta)$ for (**a**) shear-thinning and (**b**) shear-thickening liquids.

4.2 *Concentration field*

The dependence of various parameters on the concentration of the cross fluid is exhibited graphically in figures 8–10. Figures 8a and 8b are plotted to detect the characteristics of homogeneous processes k_1 on the concentration of the cross fluid. Chemically, as we increase the values of k_1, destructive chemical mechanisms increase due to which the concentration of the cross fluid deceases. The concentration profiles of the cross fluid for different values of M are shown in figures 9a and 9b. The increasing values of M result in decrease in the concentration of the cross fluid. Figures 10a and 10b show the concentration profiles of the

cross fluid for various values of Schmidt number Sc for $n < 1$ and $n > 1$. It is detected from these figures that the concentration of the cross fluid declines with elevation in Sc. From the mathematical relation of eq. (21), we detected that Sc has inverse relation with D_P. Therefore, as we increase Sc, D_P decreases due to which the concentration of the cross fluid decreases.

5. Concluding remarks

This effort scrutinised the unsteady flow of 3D cross magnetofluid under the impact of heterogeneous and homogeneous responses and nonlinear thermal radiation done by a bidirectional stretched surface. The assets of heat sink–source with convective heat transport are also deliberated. The numerical solution of the current physical problem is obtained by employing the bvp4c scheme. The somatic descriptions around the obtained outcomes were captured in this paper and the main outcomes are as follows:

- An escalation in the Biot number γ and magnetic parameter M displayed an augmentation in the liquid temperature for both $n < 1$ and $n > 1$.
- The temperature of the cross fluid decreases for increased values of magnetic parameter M. However, divergent behaviour was identified for the concentration field.
- Conflicting tendency of shear-thinning and thickening liquids of homogeneous k_1 response parameter and unsteadiness parameter S was noticed for the concentration of the cross fluid.

References

[1] M Ramzan, N Ullah, J D Chung, D Lu and U Farooq, *Sci. Rep.* **7**, 12901 (2017)

[2] M Ramzan, M Bilal and J D Chung, *PLoS ONE* **12(1)**, e0170790 (2016)

[3] Z Shafique, M Mustafa and A Mushtaq, *Results Phys.* **6**, 627 (2016)

[4] W A Khan, M Khan and A S Alshomrani, *J. Mol. Liq.* **223**, 1039 (2016)

[5] W A Khan, A S Alshomrani and M Khan, *Results Phys.* **6**, 772 (2016)

[6] T Hayat, M I Khan, A Alsaedi and M I Khan, *J. Mol. Liq.* **223**, 960 (2016)

[7] M I Khan, T Hayat, M I Khan and A Alsaedi, *Int. J. Heat Mass Transfer* **113**, 310 (2017)

[8] J V Ramana Reddy, V Sugunamma and N Sandeep, *Int. J. Eng. Res. Afr.* **20**, 130 (2016)

[9] I L Animasaun, C S K Raju and N Sandeep, *Alex. Eng. J.* **55(2)**, 1595 (2016)

[10] M I Khan, T Hayat, M Waqas, M I Khan and A Alsaedi, *J. Mol. Liq.* **233**, 465 (2017)

[11] W A Khan, M Irfan, M Khan, A S Alshomrani, A K Alzahrani and M S Alghamdi, *J. Mol. Liq.* **234**, 201 (2017)

[12] M Mustafa, J A Khan, T Hayat and A Alsaedi, *Int. J. Heat Mass Transfer* **108**, 1340 (2017)

[13] A Sohail, W A Khan, M Khan and S I A Shah, *Results Phys.* **7**, 3281 (2017)

[14] B Mahanthesh, F Mabood, B J Gireesha and R S R Gorla, *Eur. Phys. J. Plus* **132**, 113 (2017)

[15] M I Khan, M I Khan, M Waqas, T Hayat and A Alsaedi, *Int. Commun. Heat Mass Transfer* **86**, 231 (2017)

[16] M Khan, M Irfan and W A Khan, *J. Braz. Soc. Mech. Sci. Eng.* **40**, 108 (2018)

[17] M Khan, W A Khan and A S Alshomrani, *Int. J. Heat Mass Transfer* **101**, 570 (2016)

[18] M Farooq, M I Khan, M Waqas, T Hayat, A Alsaedi and M I Khan, *J. Mol. Liq.* **221**, 1097 (2016)

[19] M Atlas, Rizwan Ul Haq and T Mekkaoui, *J. Mol. Liq.* **223**, 289 (2016)

[20] N S Akbar and Z H Khan, *J. Mol. Liq.* **222**, 279 (2016)

[21] T Hayat M Waqas M I Khan and A Alsaedi, *J. Mol. Liq.* **225**, 302 (2017)

[22] M I Khan, M Waqas, T Hayat, M A Alsaedi and I Khan, *J. Mol. Liq.* **246**, 259 (2017)

[23] M K Nayak, N S Akbar, V S Pandey, Z H Khan and D Tripathi, *Powder Technol.* **315**, 205 (2017)

[24] M K Nayak, *Int. J. Mech. Sci.* **124**, 185 (2017)

[25] M Waqas, M Ijaz Khan, T Hayat, A Alsaedi and M Imran Khan, *Eur. Phys. J. Plus* **132**, 280 (2017)

[26] N Sandeep and M Gnaneswara Reddy, *J. Mol. Liq.* **225**, 87 (2017)

[27] B Mahanthesh, B J Gireesha, S A Shehzad, F M Abbasi and R S R Gorla, *Appl. Math. Mech.* **38**, 969 (2017)

[28] M M Bhatti, A Zeeshan and R Ellahi, *Pramana – J. Phys.* **89**: 48 (2017)

[29] T Hayat, M Waqas, S A Shehzad and A Alsaedi, *Pramana – J. Phys.* **86**, 3 (2016)

[30] W A Khan, M Khan, A S Alshomrani and L Ahmad, *J. Mol. Liq.* **224**, 1016 (2016)

[31] W A Khan and M Khan, *Results Phys.* **6**, 829 (2016)

[32] T Hayat, M I Khan, M Farooq, A Alsaedi, M Waqas and T Yasmeen, *Int. J. Heat Mass Transfer* **99**, 702 (2016)

[33] J V Ramana Reddy, V Sugunamma and N Sandeep, *J. Mol. Liq.* **236**, 93 (2017)

[34] M Waqas, M I Khan, T Hayat, A Alsaedi and M I Khan, *Chin. J. Phys.* **55(3)**, 729 (2017)

[35] M I Khan, M Waqas, T Hayat, M I Khan and A Alsaedi, *Int. J. Mech. Sci.* **131–132**, 426 (2017)

[36] T Hayat, M Ijaz Khan, M Waqas, A Alsaedi and M Imran Khan, *Int. J. Hydrog. Energy* **42(26)**, 16821 (2017)

[37] T Hayat, M I Khan, M Farooq, A Alsaedi and M I Khan, *Int. J. Heat Mass Transfer* **106**, 289 (2017)

[38] M Manzur, M Khan and Masood ur Rahman, *Int. J. Mech. Sci.* **138–139**, 515 (2018)